

Dynamical aspects of isotopic scaling

Martin Veselsky

Institute of Physics, Slovak Academy of Sciences,
Dubravská cesta 9, Bratislava, Slovakia
e-mail: fyzimarv@savba.sk

Abstract

Investigation of the effect of the dynamical stage of heavy-ion collisions indicates that the increasing width of the initial isospin distributions is reflected by a significant modification of the isoscaling slope for the final isotopic distributions after de-excitation. For narrow initial distributions, the isoscaling slope assumes the limiting value of the two individual initial nuclei while for wide initial isotopic distributions the slope for hot fragments approaches the initial value. The isoscaling slopes for final cold fragments increase due to secondary emissions. The experimentally observed evolution of the isoscaling parameter in multifragmentation of hot quasiprojectiles at $E_{inc}=50$ A MeV, fragmentation of ^{86}Kr projectiles at $E_{inc}=25$ A MeV and multifragmentation of target spectators at relativistic energies was reproduced by a simulation with the dynamical stage described using the appropriate model (deep inelastic transfer and incomplete fusion at the Fermi energy domain and spectator-participant model at relativistic energies) and the de-excitation stage described with the statistical multifragmentation model. In all cases the isoscaling behavior was reproduced by a proper description of the dynamical stage and no unambiguous signals of the decrease of the symmetry energy coefficient were observed.

Introduction

Multifragmentation studies in the recent years highlighted the importance of fragment yield ratios which can be used to extract thermodynamical observables of the fragmenting system such as temperature and chemical potential (for a review of related methods see e.g. [1]). In the context of isotopic distributions, the fragment yield ratios represent the details of the distribution sensitive to the isospin degrees of freedom. Similar sensitivity can be explored globally by investigating the ratio of isotopic yields from two processes with different isospin asymmetry, essentially dividing the two isotopic distributions in a point-by-point fashion. When employing the macro-canonical formula for fragment yields, such a ratio will depend on N and Z as follows [2]

$$R_{21}(N, Z) = Y_2(N, Z)/Y_1(N, Z) = C \exp(\alpha N + \beta Z) \quad (1)$$

with $\alpha = \Delta\mu_n/T$ and $\beta = \Delta\mu_p/T$, where $\Delta\mu_n$ and $\Delta\mu_p$ are the differences in the free neutron and proton chemical potentials, respectively, of the fragmenting systems. C is an overall normalization constant. Alternatively [3] the N and Z dependence can be expressed as

$$R_{21}(N, Z) = Y_2(N, Z)/Y_1(N, Z) = C \exp(\alpha' A + \beta'(N - Z)) \quad (2)$$

thus introducing the parameters which can be related to the isoscalar and isovector components of the free nucleon chemical potential since $\alpha' = \Delta(\mu_n + \mu_p)/2T$ and $\beta' = \Delta(\mu_n - \mu_p)/2T$.

An exponential scaling of R_{21} with neutron and proton numbers was observed experimentally in multifragmentation data from collisions of high energy light particles with massive target nuclei [3, 4] and from collisions between mass symmetric projectiles and targets at intermediate energies [2]. Such exponential behavior is called isotopic scaling or isoscaling [2] (the parameters $\alpha, \beta, \alpha', \beta'$ being referred to as isoscaling parameters). An isoscaling behavior was also reported in studies of heavy residues [5] and in fission data [6]. The values of the isoscaling parameters were related by several authors to various physical quantities such as the symmetry energy [2, 3], the level of isospin equilibration [5] and the values of transport coefficients [6].

As demonstrated in the literature, isoscaling appears to be a global feature of nuclear reactions and multifragmentation data and the isoscaling parameters show sensitivity to both the dynamical and the thermodynamical properties of the hot source created in the early stage of the collision. It is

of interest to clarify to which extent the isoscaling behavior is modified by the process of de-excitation in the late stage of the reaction and whether the dynamical and thermodynamical properties of the hot source can be disentangled.

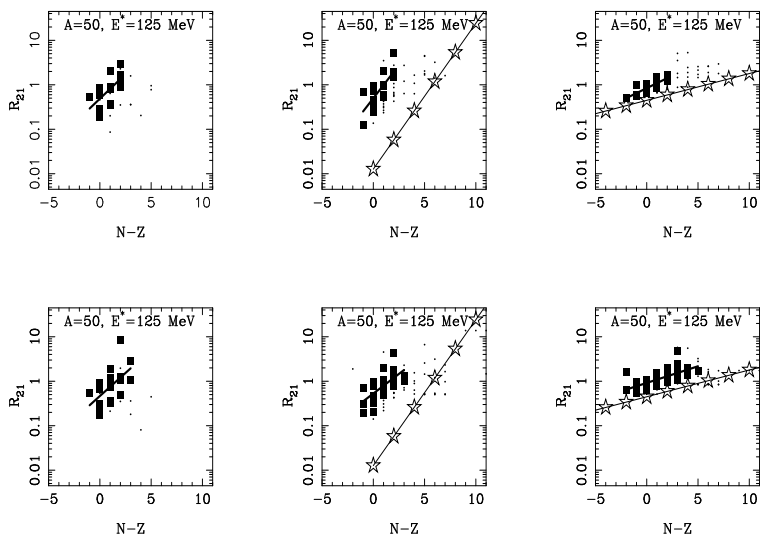


Figure 1: Isoscaling plots after de-excitation by the SMM for nuclei with mass $A = 50$ and an excitation energy of 125 MeV. Upper and lower rows represent cold and hot partitions, respectively. Squares and thick solid lines - isoscaling plots and exponential fits for $Z \leq 6$, scattered dots - all Z 's. The dynamical stage (stars connected by thin solid lines) was simulated by shifted Gaussians ($N/Z = 1.0, 1.3$) with three different values of widths ($\sigma_Z = 0.5, 2.5, 4.5$, see panels from left to right).

Effect of the de-excitation stage on isoscaling

To disentangle the dynamical and thermodynamical properties of the hot source in the experimental data and, specifically, to determine isoscaling properties after the dynamical stage, one can simulate the de-excitation process for various initial isotopic distributions produced in the dynamical stage. Such simulations allow to establish the relation between the isoscaling behavior prior to and after the de-excitation stage. In the present work the de-excitation stage is simulated using the code SMM [7], representing the

combination of the statistical multifragmentation model (SMM) for highly excited nuclei with evaporation/fission cascade at lower excitation energies. Simulations of the de-excitation stage with the SMM proved consistently better than sequential binary decay models, especially for the neutron-rich nuclides [8] and residues produced after the de-excitation of hot nuclei [9]. Some discrepancies were observed for the yields of a limited set of β -stable nuclei [8] close to the projectile, which were overestimated due to a low probability for the emission of complex fragments below multifragmentation threshold [9].

The effect of the de-excitation stage was investigated for initial (dynamical) isobaric distributions with three masses $A = 25, 50, 100$, thus covering the typical mass range where multifragmentation studies are commonly performed. In nuclear reactions, the de-excitation stage is preceded by the dynamical stage where hot nuclei are formed. An open question consists of understanding the isoscaling behavior after the dynamical stage and how it is modified by the effect of de-excitations. A possible way to answer such question is to generate the distributions of hot nuclei exhibiting isoscaling and to observe the effect of de-excitation. In order to generate the initial dynamical distributions exhibiting isoscaling one can explore the well known fact that after dividing two Gaussian distributions with equal width and shifted centers, an exponential is obtained and thus isoscaling is guaranteed. The logarithmic slope of such exponential (commonly referred to as isoscaling parameter) will thus be determined by the centers of the two Gaussian distributions, x_1 and x_2 , and their common width, σ

$$\alpha = (x_2 - x_1)/\sigma^2. \quad (3)$$

Varying of the parameters of these Gaussian distributions allows one to vary the initial isoscaling behavior at the early dynamical stage. In the present work the positions of the centers are fixed and the Gaussian width is used to control isoscaling behavior. Such a choice reflects the situation occurring in damped nucleus-nucleus collisions where the initial isospin asymmetry is not changed dramatically while the width of distribution evolves quickly with damping of the initial kinetic energy. In the simulations presented here, isoscaling after the dynamical stage was simulated using initial isotopic distributions approximated by two Gaussians with shifted centers ($N/Z = 1.0, 1.3$). Three different values of common Gaussian widths were used, $\sigma_Z = 0.5, 1.5, 3.5$ for $A = 25$ and $0.5, 2.5, 4.5$ for $A = 50, 100$. For each mass, the

yields of final products were simulated with good statistics for hot sources with five selected atomic numbers. For other elements, the yields of final products were estimated using polynomial interpolations. The calculation was carried out for two values of excitation energy, $E^* = 2.5$ and 5.0 AMeV, the former being close to multifragmentation threshold while the latter corresponding to the region where multifragmentation is the main de-excitation mode.

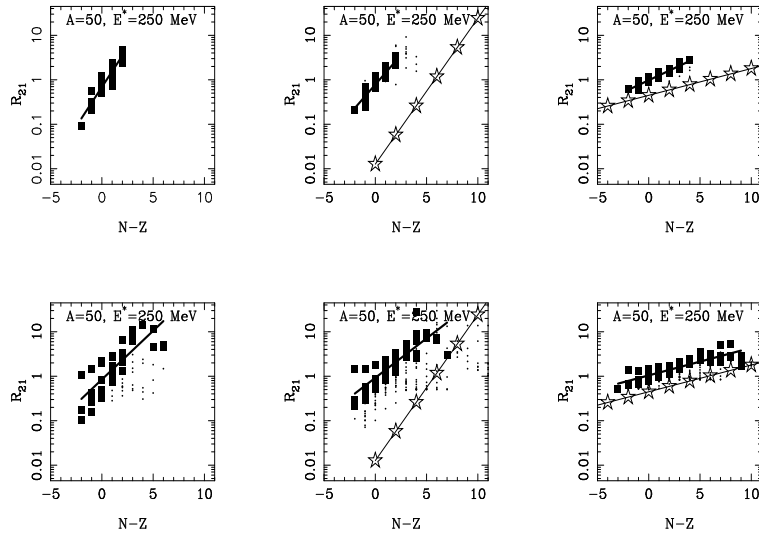


Figure 2: Isoscaling plots after de-excitation by the SMM for nuclei with mass $A=50$ and an excitation energy of 250 MeV ($\sigma_Z = 0.5, 2.5, 4.5$). Symbols and lines as in Fig. 1.

In Figs. 1, 2 are shown results for nuclei with mass $A = 50$ and excitation energies of 125 and 250 MeV, respectively. For the narrow initial Gaussian distributions (left columns) the isoscaling slopes appear to be governed by the intrinsic effect of de-excitation, while with increasing width (middle and right columns) the effect of initial distributions appears to take over. Secondary emission leads to a slight increase of the slope due to a lower temperature which, according to macro-canonical theory (Eqs. (1) and (2)), enters into the denominator. For the widest initial distribution (right columns) the isoscaling plot in the hot partition appears to follow the initial isoscaling plot and the increase of the slope by secondary emission determines the final discrepancy.

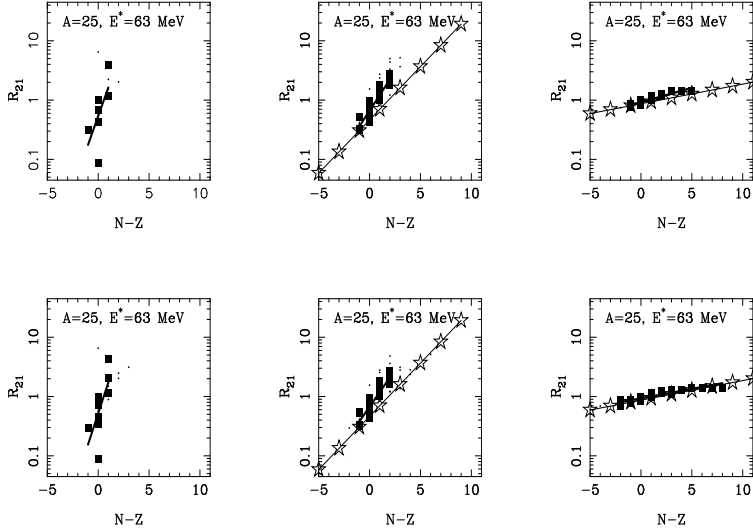


Figure 3: Isoscaling plots after de-excitation by the SMM for nuclei with mass $A = 25$ and an excitation energy of 63 MeV ($\sigma_Z = 0.5, 1.5, 3.5$). Symbols and lines as in Fig. 1.

Results for nuclei with mass $A = 25$ and excitation energies 63 and 125 MeV are shown, respectively, in Figs. 3, 4. Analogous conclusions as for $A = 50$ can be made. However, the dominance of the initial isoscaling with an increase of the slope by secondary emissions is observed in both middle and right panels, indicating that such behavior takes over earlier as the initial width increases, as compared to the case of $A=50$.

The case of $A = 100$ (excitation energies 250 and 500 MeV) is shown in Figs. 5, 6. The behavior is analogous to the previous cases, but the isoscaling slope for hot fragments with $Z \leq 6$ in the case of the widest initial distribution (lower right panel) appears to be larger than initial one. This is due to the fact that very isospin-asymmetric nuclei are produced and the symmetry energy of such light nuclei increases quickly and thus increasingly influencing the overall energy balance. However, for heavier fragments (dots) the isoscaling behavior appears to follow the initial distributions better. Such sensitivity to the symmetry energy predicted for light fragments originating from hot heavy nuclei can in principle provide a probe of the symmetry energy coefficient at the hot stage, if the reaction dynamics leads to wide initial distributions that can be reconstructed possibly via full calorimetry of the hot source or via reliable simulations of the initial stage.

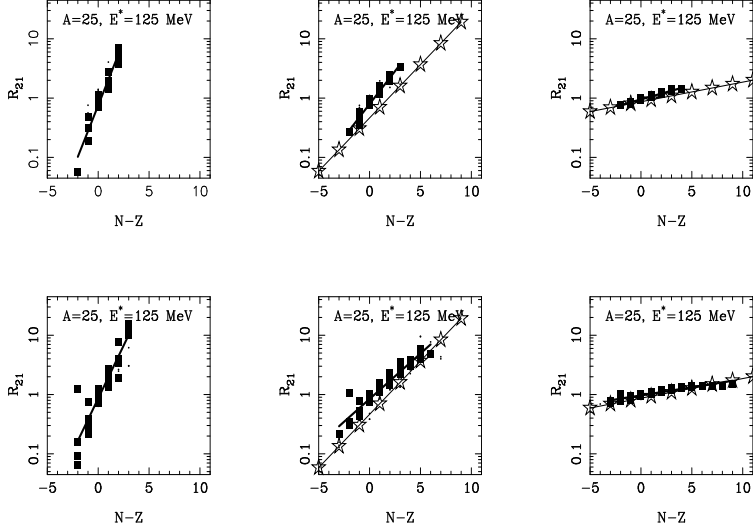


Figure 4: Isoscaling plots after de-excitation by the SMM for nuclei with mass $A=25$ and an excitation energy of 125 MeV ($\sigma_Z = 0.5, 1.5, 3.5$). Symbols and lines as in Fig. 1.

In general, the increasing width of initial isotopic distributions (and the corresponding decrease of the initial isoscaling slope) is reflected by significant modification of the final isoscaling slope after de-excitation. For narrow initial Gaussian distributions, the isoscaling slope assumes the limiting value fully determined by the details of the de-excitation stage. For wide initial Gaussian distributions, the isoscaling slope for hot fragments approaches the slope of initial isoscaling plots and it is thus fully determined by the initial stage. This correspondence is modified by secondary emission and the isoscaling slopes for final cold fragments are larger possibly due to a corresponding decrease of the temperature during secondary emissions. It is noteworthy that the width of initial Gaussian distributions induces a decrease of the isoscaling parameters comparable to the values, reported in the literature [2, 3], and explained as an effect of a decreasing symmetry energy, according to liquid-drop based formula that relates the symmetry energy coefficient directly to the isoscaling parameter. However, the effect of the dynamical stage and specifically of the width of the initial distributions was not considered in the analysis and the estimates are based on simulation for individual initial nuclei, which appears to be an over-simplified approach.

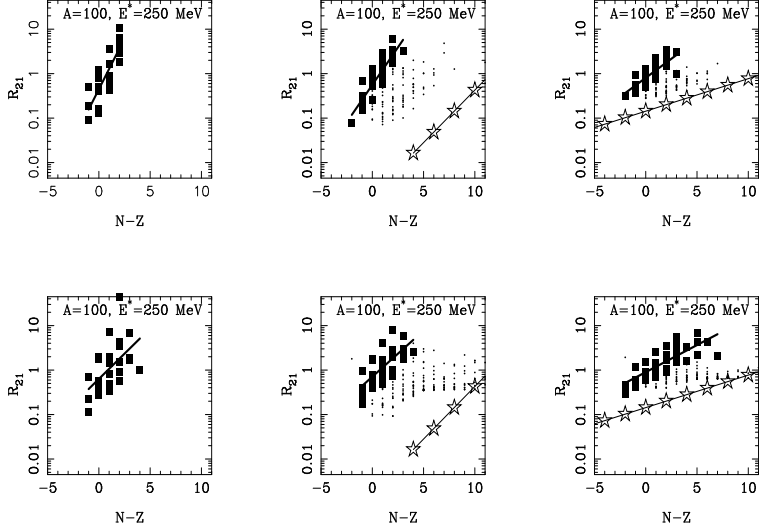


Figure 5: Isoscaling plots after de-excitation by the SMM for nuclei with mass $A = 100$ and an excitation energy of 250 MeV ($\sigma_Z = 0.5, 2.5, 4.5$). Symbols and lines as in Fig. 1.

Investigation of the dynamical stage in selected reactions

The investigation presented in previous section suggests that the dynamical stage, leading to the evolution of a considerable width of the isospin distribution, plays an important role in determining the isoscaling behavior of final products. A detailed understanding of reaction dynamics is thus necessary to allow disentangling the properties of the hot multifragmentation source from the artifacts of the reaction dynamics. Three selected cases (multifragmentation of hot quasiprojectiles at incident energy of 50 A MeV, fragmentation of a ^{86}Kr beam at an incident energy of 25 A MeV and multifragmentation of target spectators at relativistic energies) will be presented in this section in order to investigate the effects of reaction dynamics on isoscaling in few energy regions for hot nuclei with different masses.

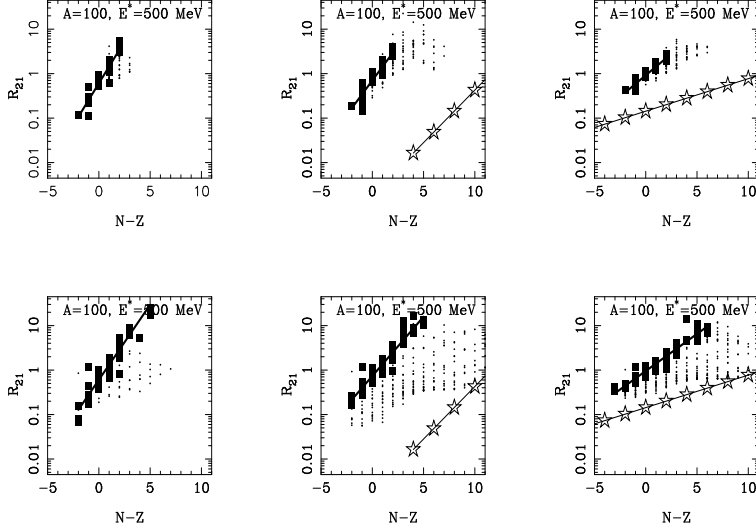


Figure 6: Isoscaling plots after de-excitation by the SMM for nuclei with mass $A = 100$ and an excitation energy of 500 MeV ($\sigma_Z = 0.5, 2.5, 4.5$). Symbols and lines as in Fig. 1.

Multifragmentation of projectiles with masses $A \sim 25$ at Fermi energies

Multifragmentation of hot quasiprojectiles with $A \sim 25$ was studied in reactions $^{28}\text{Si} + ^{124,112}\text{Sn}$ at projectile energies of 30 and 50 A MeV [10]. The observed fragment data [10] provide full information (with exception of emitted neutrons) on the decay of thermally equilibrated hot quasi-projectiles with known masses ($A = 20 - 30$), charges, velocities and excitation energies. A detailed investigation of the reaction mechanism [10] allowed to establish a dominant reaction scenario. An excellent description of fragment observables was obtained using the deep-inelastic transfer (DIT) model [11] for the early stage of the collision and the statistical multifragmentation model (SMM) [7] for the de-excitation stage. The DIT model describes well the dynamical properties of the reconstructed quasi-projectile such as its center of mass velocity, excitation energy and isospin-asymmetry. Fragment observables such as multiplicities, charge distributions and mean N/Z values for a given charge were also reproduced reasonably well [10]. Thus the reaction mechanism can be considered well understood. The contribution from non-equilibrium processes such as pre-equilibrium emission was shown to be weak

[10]. According to successful DIT+SMM simulation, the number of emitted neutrons, not detected in the experiment, was between one and two per event and the underestimation of the excitation energy due to undetected neutrons can be estimated to be approximately 10–15 % in the whole range of excitation energies. The excitation energy dependence of the isoscaling slope, corrected for the $1/T$ temperature dependence, exhibits a turning-point at $E^*=4$ AMeV [12] which can be interpreted as a signal of the onset of separation into an isospin asymmetric dilute phase and an isospin symmetric dense phase. The onset of the chemical separation is correlated to the onset of the plateau in the caloric curve, thus signaling that chemical separation is accompanied by a latent heat.

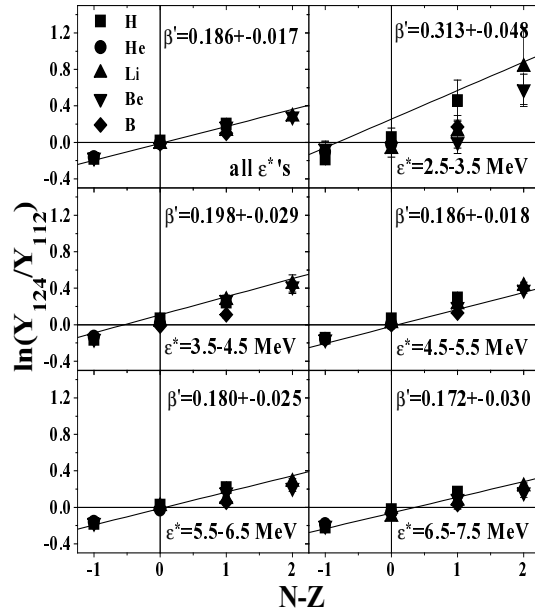


Figure 7: Simulated isoscaling plots (symbols) and fits to experimental data (lines) from the statistical decay of hot quasi-projectiles in the reactions $^{28}\text{Si}+^{124,112}\text{Sn}$ at incident energies of 50 AMeV. The upper left panel corresponds to inclusive data while the other panels correspond to the five excitation energy bins.

In Fig. 7 are presented simulated isoscaling data (symbols) from statistical decay of hot quasi-projectiles produced in the reactions $^{28}\text{Si}+^{124,112}\text{Sn}$ at projectile energy 50 AMeV. The isoscaling plots are presented not only for the inclusive data (upper left panel) but also for five bins of excitation

energy. The isoscaling slope in the simulations depends on the excitation energy almost identically as in the experimental data, represented by the solid lines. The DIT+SMM simulation fully reproduces experimental isoscaling behavior. The isoscaling parameters of the initial isospin distributions exhibit a similar trend as the final values, in agreement with the results of simulation presented in Figs. 3, 4. The shift between simulated initial isotopic distributions is constant in all the excitation energy bins and the evolution is essentially determined by their widths that are smaller in the lowest excitation energy bins and then depend on excitation energy only weakly. Despite the overall success, the simulation does not allow one to extract unambiguously the values of the temperature corresponding to isospin trends of hot fragment distributions, due to the fact that the production of multiple fragments occurs mostly in secondary emissions represented by Fermi decay. The formalism of Fermi decay is analogous to the multifragmentation model with cold fragment partitions, which thus essentially duplicates the multifragmentation model with hot fragments used in the SMM. Thus the model does not provide an unambiguous equivalent to experimental double-isotope ratio or slope temperatures, used in [12, 13]. The duplicity of fragmentation stages in the calculation is consistent with the analogous success of the model of sequential binary decay for light nuclei, where the proper exploration of available phase space appears the most important requirement to successful models.

Fragmentation of ^{86}Kr beam with $^{124,112}\text{Sn}$ targets at 25 AMeV

The isoscaling phenomena are not restricted to relatively light fragments but can be observed also in heavy residue data, collected at forward angles. Yield ratios $R_{21}(A, Z)$ of projectile residues from the reactions $^{86}\text{Kr}+^{124,112}\text{Sn}$ at 25 AMeV [14] were investigated and isoscaling behavior was observed for each isotopic and isotonic chain. The isoscaling slopes are constant for residue mass range $A = 25 - 60$, corresponding to primary events with the maximum observed excitation energy of 2.2 AMeV. The slopes exhibited gradual decrease with increasing mass of the residues. Assuming that the fragmentation occurs at normal density, using $C_{sym} = 25$ MeV [3], the values of isoscaling parameters can be used to determine the values of $\Delta(N/Z)_{qp}$ (where qp means quasi-projectile) as a function of the observed residue mass A and

charge Z , thus demonstrating the evolution of the N/Z equilibration process in isospin-asymmetric collisions. The monotonic increase of $\Delta(N/Z)_{qp}$ with excitation energy can be understood as a result of the mechanism of nucleon exchange.

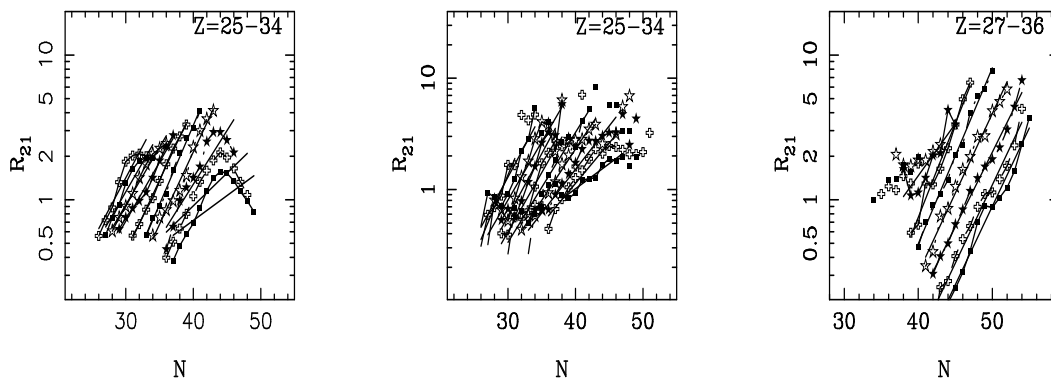


Figure 8: Isoscaling plots for the reactions of $^{86}\text{Kr}+^{124,112}\text{Sn}$ at an incident energy of 25 AMeV. Left panel - simulated data for final fragments, middle panel - experimental data [15], right panel - simulated data after dynamical stage. The lines represent exponential fits.

The left panel of Fig. 8 shows isoscaling plots corresponding to the simulations of the reactions of ^{86}Kr (25 AMeV) with $^{124,112}\text{Sn}$. The used simulation is the same as in [16] where it allowed to reproduce experimental cross sections for neutron-rich nuclides and residues from de-excitation of hot nuclei. Some discrepancies were observed in the yields of a limited set of β -stable nuclei close to the projectile, which were overestimated due to a low probability for the emission of complex fragments below multifragmentation threshold. As a comparison, in the middle panel experimental isoscaling plots are shown. For nuclei with $Z=25-30$ the simulation and experiment lead to a similar behavior with constant slopes and consistent values of the isoscaling parameters. For lower Z 's ($Z \leq 24$, not shown in the Fig. 8) the experimentally observed slopes become even larger than the calculated ones, thus eventually implying a physical phenomenon not included in the simulations, however this discrepancy can be caused by experimental limitations in measuring the yields of these elements in the tails of the isotopic distributions (as it is discussed in [16]) leading to lower widths of the isotopic distributions and thus larger apparent values of the isoscaling parameters. For heavier nuclei

with $N > 44$, the simulation leads to a reverse trend of the yield ratios toward unity, possibly signaling the onset of a reaction mechanism independent of the N/Z of the target, possibly quasi-elastic (direct) few-nucleon transfer taking place in very peripheral collisions. The experimental isoscaling behavior for these nuclei shows signs of a similar reverted trend, the transition is not as regular as in the simulation and the inclusion of the points from this region into the exponential fits (lines) leads to a decrease of the apparent isoscaling slopes. Such decrease of the slope of exponential ("isoscaling") fits is shown by the lines in the left panel of Fig. 8, despite the very poor quality of such fits. Thus the evolution of the apparent exponential slopes in both experimental and simulated data suggest a mixing of two components: one component very sensitive to the N/Z of the target, possibly due to an intense nucleon exchange; a second component, insensitive to the N/Z of the target, possibly quasi-elastic few-nucleon exchange. This situation is demonstrated in the right panel of Fig. 8 where simulated isoscaling plots are shown for the dynamical stage prior to de-excitation. The isotopes with $Z = 30 - 36$ exhibit regular isoscaling behavior, except for a structure around $N = 50$ corresponding to elements close to the projectile charge, which can be identified with quasi-elastic processes. Despite minor effect on isoscaling plots, these points represent a significant portion of the reaction cross section and the corresponding wide excitation energy distribution leads to a mixing with the data for lighter elements and thus to a modification of their isoscaling behavior after de-excitation. The discrepancy of the final simulated and experimental isoscaling behavior can be possibly attributed to an underestimated probability for the emission of complex fragments below multifragmentation threshold in the SMM.

Multifragmentation of target spectators at relativistic energies

The dominant reaction mechanism at the relativistic energies is represented by the spectator-participant model where a hot region is formed in the participant zone (zone of geometric overlap) while the spectator regions are colder. These spectators can be warm enough to undergo multifragmentation. The isoscaling behavior in multifragmentation of target spectators was investigated in the literature [4, 17] and a dependence of the isoscaling parameters on the centrality of the collision was observed [17]. The value

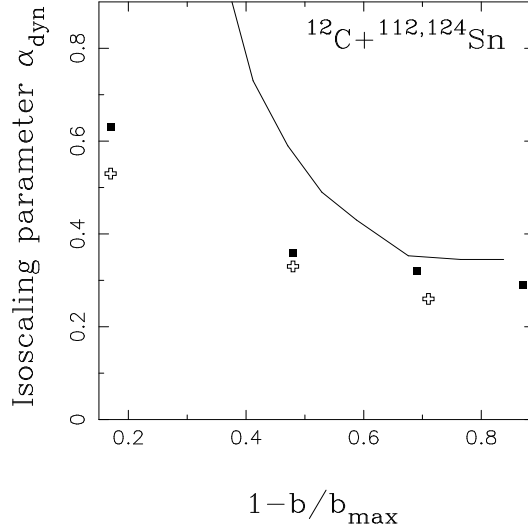


Figure 9: Evolution of the isoscaling parameter at the dynamical stage as a function of the centrality for the reactions $^{12}\text{C}+^{112,124}\text{Sn}$ at relativistic energies. Solid line - results of simulations. Symbols - experimental data [17].

of the isoscaling parameters was related to the symmetry energy [2, 3] and the decrease of the symmetry energy coefficient was reported [17]. However, based on the conclusions of the previous section, the effect of the reaction dynamics, specifically of the evolving width of the mass and charge distributions, can be considered as an alternative interpretation. The volume and thus the most probable mass A_{TS}^{abr} of the target spectator can be estimated as a function of the impact parameter using the model of geometrical abrasion [18]. The number of nucleons in the spectator zone A_{TS} can be estimated according to the binomial distribution

$$P(A_{TS}) = \binom{A_T}{A_{TS}} \left(\frac{A_{TS}^{abr}}{A_T}\right)^{A_{TS}} \left(1 - \frac{A_{TS}^{abr}}{A_T}\right)^{A_T - A_{TS}} \quad (4)$$

where A_T is the target mass number. The charge of the spectator Z_{TS} can be determined as [19]

$$P(Z_{TS}) = \frac{\binom{Z_T}{Z_{TS}} \binom{N_T}{N_{TS}}}{\binom{A_T}{A_{TS}}} \quad (5)$$

where Z_T is the target mass number and N_{TS} and N_T are the neutron numbers of the target spectator and the target, respectively. The excitation energy of the target spectator can be estimated, according to [20], as proportional to the number of abraded nucleons with the proportionality factor 27 MeV, which was found to be consistent with experimental data [21].

Fig. 9 shows the evolution of the isoscaling parameter after the dynamical stage (solid line), obtained using centers and widths of simulated fragment distributions from the abrasion calculation, as a function of centrality for the reactions $^{12}\text{C}+^{112,124}\text{Sn}$ at relativistic energies. Symbols show the experimental points reported in [17] for incident energies of 300 and 600 AMeV. The calculation is capable to reproduce the experimental trend without any assumptions about the decrease of the symmetry energy coefficient. The discrepancy at low centrality (small excitation energy) can be explained by the asymptotics of the experimental points (after the de-excitation stage) for the width approaching zero where the isoscaling parameter assumes a value determined by the intrinsic properties of the de-excitation. In central collisions the isoscaling parameter exhibits analogous saturation at a somewhat higher value (by 10 - 15 %) than the ones reported for the experimental data. The calculated widths of the target spectator isospin distributions at saturation are similar to the situation in the middle panel of Figs. 5, 6, where the initial (dynamical) isoscaling parameter reflects the initial value with remaining discrepancies due to secondary emissions. In the present case the excitation energy exceeds 11 AMeV and the effect of secondary emissions on the slope parameter in the test calculations was within statistical errors (not exceeding 10 %). Thus after taking secondary emissions into account the discrepancy will raise to the level of about 20 %, resulting in the corresponding decrease of the apparent symmetry energy coefficient from 25 MeV to about 20 MeV. Such a decrease is comparable with the uncertainty in the chosen initial values of the symmetry energy coefficient in the models of nuclear ground state properties (with the value of 23 MeV being commonly used). The decrease of the apparent symmetry energy coefficient can be further caused by other dynamical phenomena not included in the model such as emission at the pre-equilibrium stage (leading to a decrease of the shift between the centroids and to an additional increase of the widths of the isotopic distributions). The apparent value of the symmetry energy coefficient around 20 MeV can thus hardly be interpreted as a signal of a significant decrease of the nuclear symmetry energy. In any case it is much less significant than it was reported in [17] (up to factor of 6 after taking into account

secondary emissions), where the effect of the dynamical evolution of the initial isotopic distributions (the width in particular) was not considered. The model description of the dynamical evolution presented here thus allows one to reproduce the reported discrepancy, with the remaining discrepancies on the apparent symmetry energy coefficient being not significant enough to be declared as an unambiguous signal.

Summary and conclusions

Investigation of the effect of the dynamical stage of heavy-ion collisions established that the increasing width of the initial isotopic distributions induces a significant modification of the isoscaling slopes after the de-excitation stage. For narrow isotopic distributions, the isoscaling slope assumes the limiting value for two individual initial nuclei which is fully determined by the details of the de-excitation. For wide initial isotopic distributions, the isoscaling slope for hot fragments approaches the initial isoscaling slope and it is thus fully determined by the initial stage. This correspondence is modified by secondary emissions and the isoscaling slopes for final cold fragments are larger by an amount possibly corresponding to a lowering temperature during secondary emissions. The decrease of the isoscaling parameters, caused by the increase of the width of initial Gaussian distributions, is comparable in magnitude to the values, reported in the literature as an effect of the decrease of the symmetry energy. The experimentally observed evolution of the isoscaling parameter in the statistical decay of hot quasiprojectiles from the reactions $^{28}\text{Si}+^{124,112}\text{Sn}$ at projectile energy 50 AMeV is reproduced by a simulation with the dynamical stage described by the deep inelastic transfer model and the de-excitation stage described using the statistical multifragmentation model. The evolution of the apparent isoscaling slopes in both experimental and simulated data for projectile residues from the reactions of $^{86}\text{Kr}+^{124,112}\text{Sn}$ at incident energies of 25 AMeV suggests a mixing of two components, one sensitive to the N/Z of the target, possibly due to an intense nucleon exchange, and a second component due to a quasi-elastic few-nucleon exchange, almost insensitive to the N/Z of the target. The discrepancy between the final simulated and experimental isoscaling behavior can be possibly attributed to the absence of a mechanism for the emission of complex fragments below multifragmentation threshold in the SMM. The decrease of the isoscaling parameter in the multifragmentation of target spectators in

central collisions was reproduced using the simulation using the spectator-participant model for the dynamical stage and the SMM model for the de-excitation stage. In all cases the isoscaling behavior was reproduced by a proper description of the dynamical stage and no unambiguous signals on the decrease of the symmetry energy coefficient were observed.

The author acknowledges L. Tassan-Got for providing his DIT code and A.S. Botvina for providing his SMM code. This work was supported through grant of Slovak Scientific Grant Agency VEGA-2/5098/25.

References

- [1] M. Veselsky, *Fiz. Elem. Chastits At. Yadra* 36, 400 (2005); *Physics of Part. and Nuclei* 36, 213 (2005).
- [2] M.B. Tsang et al., *Phys. Rev. Lett.* 2001. V.86. P.5023.
- [3] A.S. Botvina et al., *Phys. Rev. C.* 2002. V.65. P.44610.
- [4] O.V. Lozhkin, W. Trautmann, *Phys. Rev. C.* 1992. V.46. P.1996.
- [5] G.A. Souliotis et al., *Phys. Rev. C.* 2003. V.68. P.24605.
- [6] M. Veselsky, G.A. Souliotis, M. Jandel, *Phys. Rev. C.* 2004. V.69. P.44607.
- [7] J.P. Bondorf et al., *Phys. Rep.* 1995. V.257. P.133.
- [8] M. Veselsky, G.A. Souliotis, *Nucl. Phys. A* 765 (2006) 252.
- [9] M. Veselsky et al., *Nucl. Phys. A.* 2003. V.724. P.431.
- [10] M. Veselsky et al., *Phys. Rev. C.* 2000. V.62. P.064613.
- [11] L. Tassan-Got, PhD Thesis, 1988, Orsay, France, IPNO-T-89-02, 1989; L. Tassan-Got, C. Stéfan, *Nucl. Phys. A.* 1991. V.524. P.121.
- [12] M. Veselsky, G.A. Souliotis, S.J. Yennello, *Phys. Rev. C.* 2004. V.69. P.31603(R).
- [13] M. Veselsky, S.J. Yennello, *Nucl. Phys. A* 749, 114c (2005).

- [14] G.A. Souliotis et al., Phys. Lett. B. 2004. V.588. P.35.
- [15] G.A. Souliotis et al., Phys. Rev. Lett. 91 (2003) 022701.
- [16] M. Veselsky, G.A. Souliotis, arxiv.org:nucl-th/0607032.
- [17] A. Le Fevre et al., Phys. Rev. Lett. 94, 162701 (2005).
- [18] J. Gosset *et al.*, Phys. Rev. **C 16** (1977) 629.
- [19] W.A. Friedman, Phys. Rev. **C 27** (1983) 569.
- [20] J.-J. Gaimard, K.-H. Schmidt, Nucl. Phys. **A 531** (1991) 709.
- [21] K.-H. Schmidt et al., Phys. Lett. **B 300** (1993) 313.